Dispersion correction in DCE-MRI microvascular parameters using a recirculating bolus AIF model

R. A. Little[1], M. Scott[2], A. Banerji[1], Y. Watson[1], J. Naish[1], and G. J. Parker[1]
[1]Imaging Sciences & Biomedical Engineering, University of Manchester, Manchester, United Kingdom, [2]AstraZeneca, Cheshire, United Kingdom

Introduction: A common assumption made when analysing dynamic contrast-enhanced MRI (DCE-MRI) data is that negligible dispersion occurs between the arterial input function (AIF) measurement site and the tissue of interest. Any such dispersion may result in errors in the derived microvascular parameters of interest. Local AIFs have been derived based on relationships between the tracer uptake in the tissue of interest and reference regions [1] and through blind estimation from the tissue of interest alone [2]. These methods typically assume that there is a single input function relating to the signal changes across the tissue of interest. In neoplastic tissue, it may be that the underlying input function varies between tumour regions and therefore voxels as a consequence of multiple tortuous paths of travel resulting from disordered vessel growth. Here we consider whether it is feasible to model dispersion using a functional form of an AIF and, using the extended Kety model, measure both the level of dispersion and correct the measured parameters of interest for such dispersion on a voxelwise level.

$$\gamma(A,\alpha,\beta,t_p) = \frac{A}{\beta^{\alpha+1}\,\Gamma(\alpha+1)}(t+\alpha\beta-t_p)^{\alpha}e^{-\frac{(t+\alpha\beta-t_p)}{\beta}},\ 0\le t<\infty,\ \alpha>-1 \qquad (Eq\ 1)$$

$$C(t) = \gamma(A_1+A_2,\alpha_1,\beta,\mu) + \sum_{j=1}^{\infty}\gamma\left(A_1e^{-m_1j\rho}+A_2e^{-m_2j\rho},\ j\alpha_2+2j-2,\ \beta,\ \mu+j\rho\right) \qquad (Eq\ 2)$$

$$\alpha' = \alpha + d((2\alpha+2)-\alpha) \qquad (Eq\ 3)$$

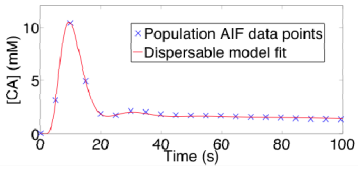

Fig 1: A dispersable recirculating bolus model fit to the Parker population AIF.

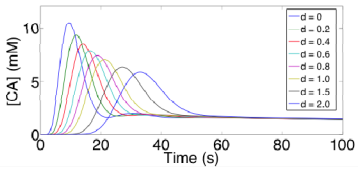

Fig 2: The set of candidate dispersed AIFs used for the model fits resulting from applying dispersion factors d *to the Parker population AIF*

Methods: ***Theory*** A functional form for the AIF was derived based on the recirculating bolus model of Horsfield *et al.* [3]. In order to allow the individual gamma variate models of the recirculating bolus to be dispersed by modification of the (variable) α term, our model considers the exponential decay to act on the area inside each bolus rather than on the entire function. If each recirculating bolus is described by a gamma variate $\gamma(A, \alpha, \beta, t_p)$ (Eq. 1) then the model may be described by Eq. 2, where A represents area, α and β parameterise the gamma variate, t_p is the peak time of the gamma variate, Γ is the gamma function, A_n is the area under pass n, m_1 and m_2 are the area decay parameters, α_n is the α parameter for pass n, μ is the peak time of the first pass and ρ is the time between each peak. An initial model of dispersion of each individual pass of the bolus was provided by modifying α to α' according to Eq. 3, where d represents dispersion as a fractional value between that of the measurement and a modelled recirculation. ***Simulations*** Tissue concentration time courses were simulated using the extended Kety model for each combination of the given parameters v_p = 0.0018, 0.01, 0.09, 0.18, K^{trans} = 0.05, 0.20, 0.35, 0.50 min^{-1}, and v_e = 0.30 and various adaptations of an accepted model of the AIF, as detailed below. For every combination, 100 samples at a 5 s temporal resolution were generated by applying normally distributed noise (SD 0.07 mM). Simulated uptake curves were generated and fitted under four sets of conditions: (A) generated using the Parker population-averaged AIF (PAIF) [4] with no dispersion and fitted without incorporating dispersion ('baseline'); (B) generated using the PAIF dispersed by fraction 0.4 and fitted using the standard process ('standard fit to data with dispersion'); (C) generated using the PAIF with no dispersion and fitted by searching for the lowest model error using all the candidate AIFs of Fig 2 ('dispersed model fit for data with no dispersion'); (D) generated using the PAIF dispersed by fraction 0.4 and fitted using all the candidate AIFs as before ('dispersed model fit for data with dispersion'). ***Patient Data*** DCE-MRI parameters were fitted for a liver metastasis from a single, central slice from a primary colorectal tumour similarly to (C) and (D) above except that d was allowed to vary freely during the fitting. The PAIF was used for the fitting with the candidate functions of Fig 2.

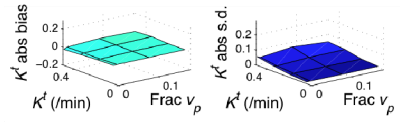

Fig 3: Bias and SD of K^{trans} errors for baseline conditions (A).

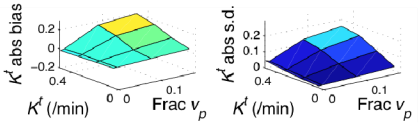

Fig 4: Bias and SD of K^{trans} errors for standard fit to data with dispersion (B).

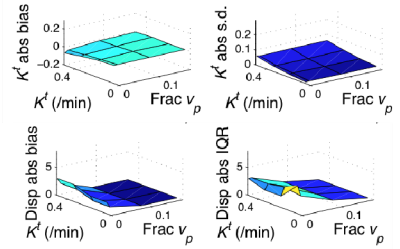

Fig 5: Bias and SD/IQR of K^{trans} and dispersion errors for dispersed model fit for data with no dispersion (C).

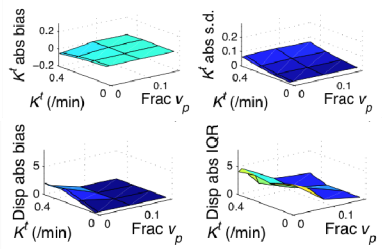

Fig 6: Bias and SD/IQR of K^{trans} and dispersion errors for dispersed model fit for data with dispersion (D).

Results: Fig 1 demonstrates a model fit to the PAIF and Fig 2 shows the result of applying a model of dispersion to this fit over the early part of the time series. Figs 3-6 show the simulation results in the form of absolute bias from the true value and the standard deviation or interquartile range of the simulation samples for K^{trans} and dispersion. Not accounting for dispersion when present leads to large errors (Fig 4). Incorporating dispersion of the AIF into the fitting substantially reduces these errors when dispersion is present (Fig 6) and does not cause bias when dispersion is absent (Fig 5). v_e and v_p showed similar trends and these were similarly corrected for by the dispersion modelling. Fig 7 shows a mean 11 % tumour K^{trans} decrease as a result of incorporating dispersion. Fig 8 shows the fitted dispersion parameter across the tumour, which had a mean value of 3.4.

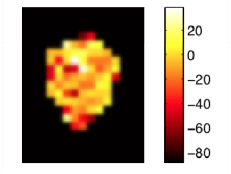

Fig 7: Percentage change in K^{trans} from standard model across region of interest.

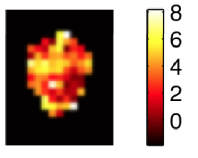

Fig 8: Fitted dispersion factor across region of interest (no units).

Discussion and Conclusion: The AIF model form provides a precise fit to the PAIF (Fig 1) data and could be applied to individually measured AIFs. The model allows the fitted AIF to be dispersed and simulations show that extended Kety parameters can be extracted from the data along with the level of dispersion of the input function. The tumour data demonstrate a reduction in mean K^{trans} and the possibility of modelling dispersion at the voxel level. This dispersion term may also be influenced by capillary level effects due to a finite transit time and so may generally describe the effects of flow related dispersion on tracer kinetics. The results suggest that, where AIFs undergo dispersion, tracer kinetic parameters will show bias and reduced precision if dispersion is not considered; however, with appropriate modelling, it appears possible to reduce such errors, as well as estimate dispersion, which may be a parameter of interest in its own right.

[1] Yankeelov *et al.*, MRM, 57:353-361, 2007; [2] Schabel *et al.*, Phys Med Biol, 55:4783-4806, 2010;
[3] Horsfield *et al.*, Phys Med Biol, 54:2933-2949 (2009); [4] Parker *et al.*, MRM 56:993-1000, 2006.

The authors are grateful to AstraZeneca for their partial funding of this work and to Gordon Jayson for patient recruitment.